Factors affecting the accuracy of population balance solutions in immiscible systems

G. Polprasert, A.M. AlTaweel, J.R. Webber, R.C. Devavarapu and P. Gupta
Chemical Engineering Department, Dalhousie University, Halifax NS, Canada
A.S.I. Elsayed
Eng. Mathematics and physics Dept., Faculty of Engineering, Alexandria University, Alexandria, Egypt
K. Prabriputaloong and C. Tangsatitkulchai
Suranaree University of Technology, Nakhonratchasima, Thailand

The coalescence and breakage of drops in turbulent flows strongly influences the rate of inter-phase heat and mass transfer achievable in multi phase contacting devices. Accurate modeling of these processes is therefore a necessary component in any realistic description of the complex interactions taking place in such units. Unfortunately, the accuracy of the technique most commonly used in such situations (population balance techniques) has rarely been investigated. The errors encountered in solving Population Balance (PB) simulations can be attributed to the following: (1) errors resulting from the numerical solution of the integro-differential PB equations, (2) errors resulting from the over-simplified representation of the complex hydrodynamics encountered in mechanically agitated tanks, (3) indiscriminate use of coalescence/dispersion models under conditions where they may not be applied. This work was consequently undertaken with the objective of determining the effect of various factors on the accuracy of the results obtained. Depending on the size of integration time interval, drop size increment, solution method, and the breakage/ coalescence rates, errors as high as 230% in the average equilibrium drop size were observed. On the other hand, order of magnitude errors were encountered when inappropriate collision frequency models are used. Based on the findings obtained, a user-friendly algorithm capable of accurately solving PB equations was developed. This resulted in reducing the error down to less than 1% without significantly increasing computational time.

عمليات التكسر والالتحام لقطرات السائل المنتشر تحت ظروف السريان الاضطرابي ، تؤثر في معدلات انتقال الحرارة والكتله في المفاعلات المتعددة الأطوار. التمثيل الصحيح لهذه العمليات ضروري لوصف التفاعلات المعقدة داخل هذه المفاعلات وصفا صحيحا. ويستخدم نموذج الاتزان العددي لتحليل وتصميم المفاعلات الكيمائية المتعددة الأطوار آخذا في الاعتبار عمليات التكسر والالتحام. لم تدرس دقة هذا النموذج الدراسة الكافية، حيث أن هناك أخطاء تنشأ في حل نموذج الاتزان العددي من التمثيل المبسط جدا للعمليات الهيدروديناميكية المعقدة واستخدام نماذج التكسر والالتحام في غير موضعها. هذا البحث هو استكمال لدراسة العوامل التي تؤثر على صحة النتائج المستخرجة من حل نموذج الاتزان العددي. وهذه العوامل هى حجم الفترة الزمنية وفترة زيادة حجم القطرات وطريقة الحل المستخدمة ومعدلات التكسر والالتحام. وقد وجد أن استخدام النموذج الرياضي الغير مناسب لعمليات التكسر والالتحام يؤدي الى خطأ في النتائج. وقد أظهرت النتائج أنه يجب تعديل حجم الفترة الزمنية وفترة زيادة حجم القطرات تبعا لمعدلات التكسر والالتحام وذلك للحصول على نتائج دقيقة. بناءا على هذه الدراسة تم عمل نظام حسابي قادر على حل نموذج الاتزان العددي بدقة. وقد قلل هذا الأسلوب الخطأ لأقل من ١% بدون زيادة تذكر في وقت الحساب.

Keywords: Population balance model, Breakage and coalescence processes, Drop/bubble size distribution, Multiphase systems, Mixing processes

1. Introduction

The multi-phase flow appears in many engineering operations such as chemical, petroleum, mining, food, and pharmaceutical industries. The reaction and mass transfer processes occurring in these systems are of major importance. Thus, the knowledge of the dispersion phenomena such as interfacial area, particle size and residence time distributions, and dispersed phase breakage and coalescence rates, are important for a reliable design purposes. Breakage and coalescence processes can profoundly influ-

ence the overall performance of the contactors, by altering the interfacial area available for mass transfer. Fig. 1 describes the role of breakage and coalescence in multi-phase systems. Most often the criteria for reactor and extractor design are empirical and the scale-up involves costly experimental programs. A major reason for empirical analysis is the inability to describe dispersion properties such as the droplet size distribution, interfacial surface area, and droplet mixing rates as a function of the agitation rate and physical parameters. The population balance approach is employed for the description of droplet dynamics in various flow fields. A significant advantage of the method is that a vehicle is provided to include the details of the breakage and coalescence processes in terms of the physical parameters and condition of operation. Solution of the population balance equation enables prediction of instantaneous drop size distribution that, in turn, may be used to describe in more detail the hydrodynamics and mass transfer rates in a given system.

After simplifying the complicated integro-differential Population Balance Equation (PBE) by making the suitable assumptions, the suitable method must be chosen so that it gives accurate results, which should fit well the experimental results. Except in certain simplified situations, it is not often that analytical solutions can be found for PBE. Sovova [1], and Rod and Misek [2] derived exact solution for the PBE in a batch mixer, assuming simple power functions in drop size for breakage and coalescence. Generally, PBE requires numerical solution. Lee et al. [3] applied the population balance equation coupled with the proposed breakage kernel and the previously developed breakage model to the analysis of bubble size distribution for non-coalescing systems in a bench-scale airlift column. They solved the steady-state population balance equation using Simpson's integration technique. Niyogi et al. [4] solved the population balance equation numerically using adaptive fourth-order Runge-Kutta method. Chatzi et al. [5] described the steady-state drop size distribution in a batch stirred vessel by PBE. They solved PBE using composite Simpson's rule.

The objective of the present work is to develop a user friendly population balance program capable of accurately simulating multi-phase contactors, accurate numerical solution, better representation of the hydrodynamics of industrial units, and having modeling flexibility for various sub-components.

2. Mixing research at Dalhousie University

In a Pneumatically agitated contactors such as bubble column fig. 2, the energy necessary for agitation input to the system through the gas, which has the energy necessary to agitate the continuous phase. The gas enters the column through sparger

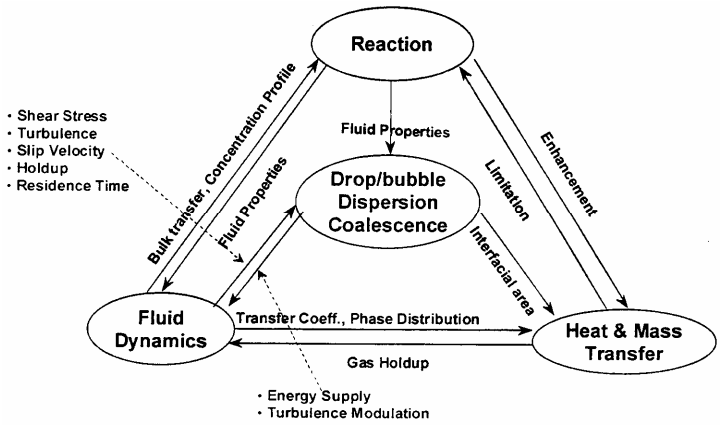

Fig. 1. Role of breakage and coalescence in multi-phase systems.

(Venturi) in the column bottom and rise to the column top, agitating the liquid inside the column. During the gas rising process in the column, the gas bubbles undergo different breakage mechanisms such as laminar, buoyancy, and turbulence breakage mechanism. The energy cascading from the gas to the liquid agitates the liquid phase and creates turbulent eddies in it. These eddies bombard the bubble surface, if they overcome the surface energy of the bubble, the bubble will breakup. Also, turbulence motion may lead to coalescence. Thus, it is necessary to calculate the energy dissipation rate for the gas phase inside the column, to use it in calculating bubbles breakage and coalescence rates.

3. Population balance equation

In a dispersed phase system, the material domain comprises a continuous phase and a dispersed phase, the latter as a population of particles (drops, bubbles, or solid) in which the identities of individuals are continually destroyed and recreated by breakup and coalescence processes. Considering the control volume in fig. 3. The population balance model is based on an equation for the continuity of particle numbers in a dispersed phase and is developed from the general conservation equation.

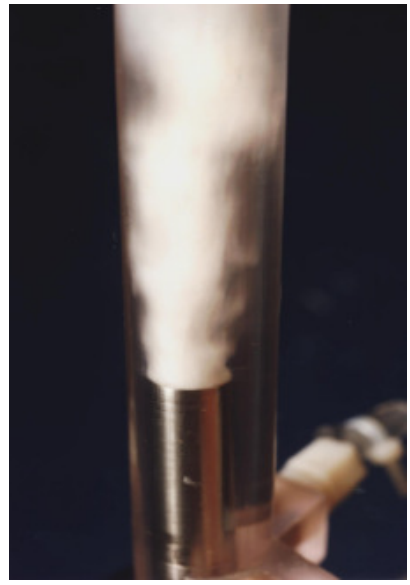

d_{32}=300 μm (Sauter mean diameter)
U_L=1m/s (Superficial liquid velocity)
U_G (Superficial gas velocity)/U_L (Superficial liquid velocity)=0.3
20 ppm MIBC

Fig. 2. Gas-sparged bubble column.

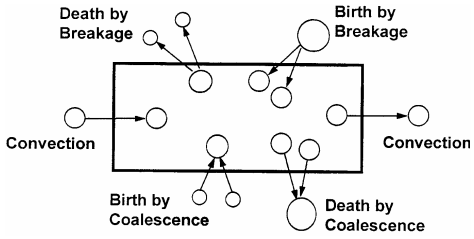

Fig. 3. Control volume.

Accumulation rate = flux in (convection and diffusion) – flux out + Net generation rate. (1)

Consider the distribution of entities $n(r, \xi_1, \xi_2,\ldots, \xi_m, t)$ or the population of particles of the dispersed phase at position r, where r represents the spatial coordinates or "external coordinates", t is the time, and ξ_i represents the i th other property of the entity. ξ_i is also called the internal coordinate and used to give a quantitative description of the state of an individual particle, such as its mass, concentration, temperature, age, volume, etc. In addition to time, there are (3+m) independent variables involved that can be thought of as a (3+m) dimensional space.

The PBE in its most general form [6] is:

$$\frac{\partial n}{\partial t} + \nabla\bullet(\overline{V} \cdot n) - B + D = 0, \quad (2)$$

where $\overline{V}$ is the coordinate velocity in phase space. For well-mixed batch mixing tank, with no reaction or heat/mass transfer, the problem simplifies to the following two-dimensional situation [7]

$$\frac{d\,[N(t)\,f(a,t)]}{d\,t} = B_B(a,t) - D_B(a,t) + B_C(a,t) - C(a,t), \quad (3)$$

where N(t) is the total number of particles at time t. f(a,t) is the fraction of particles have diameter between a and a+Δa. $B_B(a,t)$, $D_B(a,t)$, $B_C(a,t)$, and $D_C(a,t)$ are the birth rate by breakage, death rate by breakage, birth rate by coalescence, and death rate by coalescence, of particles of diameter a at time t, respectively.

3.1. Breakage rate

Breakage results in both "death" as well as "birth" within a certain drop size range.

$$B_B(a,t) = \int_a^{a_{max}} \beta(a,a')\, \varsigma(a')\, \Omega(a')\, N(t)\, f(a',t)\, da', \quad (4)$$

$$D_B(a,t) = \Omega(a)\, N(t)\, f(a,t). \quad (5)$$

From eqs. (4, 5), the breakage rate is affected by [8]:
i- breakage frequency $\Omega(a)$, which is function of energy dissipation rate per unit mass ε, surface tension σ, density of dispersed phase ρ_D, density of continuous phase ρ_C, viscosity of dispersed phase μ_D, and viscosity of continuous phase μ_C,
ii- number of daughter drops $\varsigma(a)$, where $\varsigma(a')$ may be (2,3,4,...),
iii- size distribution of daughter drops $\beta(a,a')$, where $\beta(a,a')$ is assumed (equi-sized, Normal, Gamma, Beta,...).

3.2. Coalescence rate

Coalescence results in both "death" as well as "birth" within a certain drop size range.

$$B_C(a,t) = \int_0^{a/2} \lambda(a-a', a')\, \omega(a-a', a')\, N(t)\, f(a-a',t) N(t)\, f(a',t)\, da', \quad (6)$$

$$D_C(a,t) = N(t)\, f(a,t) \int_0^{a_{max}-a} \lambda(a, a')\, \omega(a, a')\, N(t)\, f(a',t)\, da'. \quad (7)$$

Here, $\lambda(a, a')$ is the coalescence efficiency between drops of size a and a', and $\omega(a, a')$ is the collision frequency between drops of size a and a'. From Eqs. (6,7), the coalescence rate is affected by [8]:
i- collision frequency $\omega(a, a')$, which is function in energy dissipation rate per unit mass ε, density of dispersed phase ρ_D, density of continuous phase ρ_C, and diameters of colliding drops (a, a'),
ii- coalescence efficiency $\lambda(a, a')$, which is defined as the fraction of collisions between drops of diameter a and a' that result in coalescence. It is function of contact time between drops and coalescence time which is the time required for drops to coalesce.

3.3. Accuracy of population balance formulation

Fig. 4 shows comparison between analytical solution of Rod and Misek [2], and numerical solution using fixed time interval $(\Delta t = 2s, 3s, 4s, 5s, and\ 6s)$. As the time interval increases, the error and divergence from analytical solution increase.

3.4. Errors in population balance formulation

i- Disregard of the large spatial variation in energy dissipation rate (ε). The energy dissipation rate determines the drop/bubble size distributions in the contactor through controlling the breakage and coalescence processes. In addition, the energy dissipation rate evaluates the system efficiency in utilizing energy input to the system through mechanical or pneumatical methods. In the mechanically agitated tank fig. 5, the energy input to the system through mechanical device such as impellers. Due to the lack of information for the variation of ε in the stirred tank, ε is commonly determined by taking the total volume as the energy dissipation volume (average value). In view of the significant inhomogeneities existing in the stirred tank reactor fig. 5, it may not be reasonable to use average value for ε.
ii- Emphasis on binary breakage, $\varsigma(a')=2$. Experiments show that breakage of drop results in various numbers and sizes of daughter drops. Most investigators assume a fixed number of daughter drops to simplify the computation. Various investigators used the value $\varsigma(a')=2$ in their models [8].
iii- Presence of large numbers of models describing the various sub-processes (often conflicting), e.g., there are different models

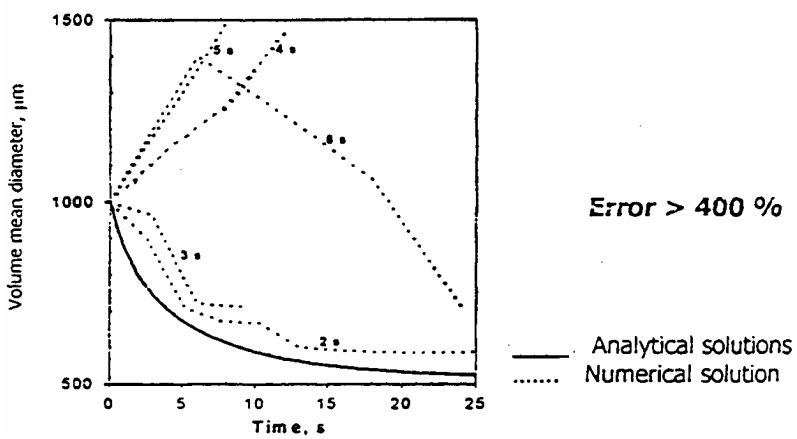

Fig. 4. Effect of fixed time interval on numerical solution.

describe the functions of collision frequency $\omega(a, a')$, coalescence efficiency $\lambda(a, a')$, breakage frequency $\Omega(a)$, and size distribution of daughter drops $\beta(a,a')$.

iv- Lack of experimental data in which coalescence or breakage mechanisms dominate (to discriminate amongst the various sub-processes).

v- Lack of information on the factors affecting the accuracy of numerical solutions.

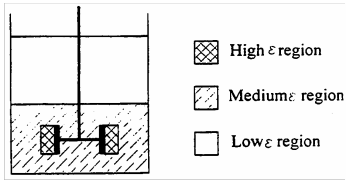

Fig. 5. Batch mixer (agitated tank).

3.5. Project objectives

To develop a user friendly PB program capable of accurately simulating multi-phase contactors:

i- accurate numerical solution,

ii- better representation of the hydrodynamics of industrial units,

iii- having modeling flexibility for various sub-components.

4. The Rod and Misek analytical solution

Rod and Misek [2] obtained an analytical solution for the transient and equilibrium drop diameters by assuming simple power functions for breakage and coalescence processes, expressed by:

$$\Omega(a') = K_s\, a^{3(p+1)}, \tag{8}$$

$$\beta(a,a') = 3\, a^2/a'^3, \tag{9}$$

$$\varsigma(a') = 2, \tag{10}$$

$$\lambda(a-a', a')\, \omega(a-a', a') = K_c\, (a^3 + a'^3)^p\ , \tag{11}$$

where K_s and K_c are the breakage and coalescence rate constants. The analytical solution of the steady-state PBE using the above models, leads to the steady-state drop number density:

$$f(a) = \frac{3\,a^2}{\bar{a}^2}\ \exp\left[-\left(\frac{a}{\bar{a}}\right)^3\right]. \tag{12}$$

Mean volume drop diameter $\bar{a}$, as the parameter of the distribution, is given by:

$$a = \left(\frac{3}{\pi}\ \frac{K_c\,\phi}{K_s}\right)^{1/6}, \tag{13}$$

where ϕ is the volume fraction of the dispersed phase. The transient distribution developing during the transition from one steady state, characterized by the mean volume diameter $\bar{a}_o$ to another steady state, characterized by

the mean volume diameter $\bar{a}_\infty$, can be described by:

$$f(a,t) = \frac{3\,a^2}{[\bar{a}(t)]^3}\ exp\,[-(a/\ \bar{a}(t))^3]\ . \qquad (14)$$

The time variation of the value $\bar{a}$, depending on the exponent p, is described by differential equation,

$$\frac{d\,\bar{a}}{d\,t} = \frac{\Gamma(p+2)}{3} K_s\ \ \bar{a}^{3p-2}\,(\ \bar{a}_\infty^{\,6} - \ \bar{a}^{6}). \qquad (15)$$

The solution of eq. (15), for p=0, has the form;

$$\bar{a}(t) = \bar{a}_\infty \left(\frac{1 + A\,exp\,(-2\,K_s\,\bar{a}_\infty^{\,3} t)}{1 - A\,exp\,(-2\,Ks\,\bar{a}_\infty 3t)}\right)^{1/3}, \qquad (16)$$

where

$$A = \frac{\bar{a}_0^{\,3} - \bar{a}_\infty^{\,3}}{\bar{a}_0^{\,3} + \bar{a}_\infty^{\,3}}. \qquad (17)$$

The analytical solution of Rod and Misek [2] was used to identify the factors controlling the accuracy of numerical solutions and develop algorithms that can minimize them. The rate at which equilibrium is achieved depends on the value of the coalescence and breakage rate constant (K_c & K_s).

Fig. 6 shows the effect of sudden variation in the RPM of the impeller, on the volume mean diameter in the batch mixer.

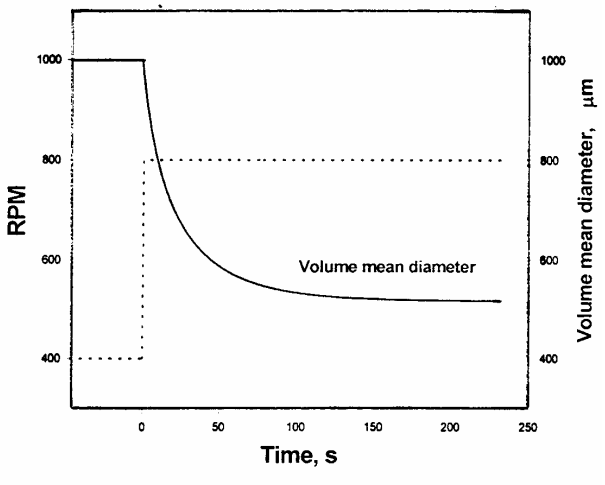

Fig. 6. Effect of RPM on volume mean diameter.

5. Sources of error in numerical solutions

i- discretization errors (time and size domains),
ii- truncation errors (approximating exact mathematical procedures),
iii- roundoff errors (inexact representation of floating point numbers),
iv- propagated errors (errors from previous steps carried through to succeeding steps),
v- when is quasi-steady state reached?, the quasi-steady state means that the mean diameter of the drops stop changing with time any more, meanwhile breakage and coalescence processes still working.

6. Quasi-equilibrium state approach

The quasi-steady state means that the mean diameter of the drops stop changing with time any more, meanwhile breakage and coalescence processes still working. The transition from one steady state, characterized by the mean volume diameter $\bar{a}_o$ =1000 µm to another steady state, characterized by the mean volume diameter $\bar{a}_\infty$ =1445 µm, is described in fig. 7. The error in calculating the equilibrium volume mean diameter at points 1, 2 and 3, is 5.7 %, 4.2 % and 1.4 %, respectively.

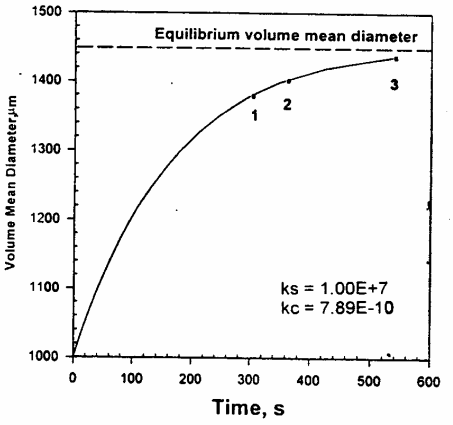

Normalized quasi-steady state tolerance

$$\left(\frac{\Delta a}{a}\frac{t}{\Delta t}\right)$$

1: 0.24 (5.7 % error)
2: 0.15 (4.2 % error)
3: 0.053 (1.4 % error)

Fig. 7. Quasi-steady state approach.

6.1. Using fixed step size in the time domain

Fig. 8 shows the percentage error in calculating the equilibrium volume mean diameter numerically, using fixed time step size. As the time step size increases, the error increase, and the computing time decrease. The constants of the breakage and coalescence rates are, *ks*=1.0E+8, and *kc*=2.0E-11, respectively.

Fig. 9 shows comparison between analytical and numerical solution for the variation of the volume mean diameter with time. The time interval Δt=15 s. As the *ks* increases, the time interval must decrease to decrease the error in the numerical solution.

6.2. Using adaptive step size in the time domain

Fig. 10 shows comparison between analytical and numerical solution for the variation of the volume mean diameter with time, using Runge-kutta 4th order with adaptive step size. The numerical solution are shown to be coincide with analytical solution of Rod and Misek [2].

7. Components of the net generation term

The birth by breakage (eq. (4)), death by breakage (eq. (5)), birth by coalescence (eq. (6)), and death by coalescence (eq. (7)), are calculated and represented in fig. 11. The round off error is reduced by limiting the calculation of birth and death rates, i.e. using suitable values *for* $a_{max,BC}$, $a_{max,BB}$, $a_{max,DC}$, and $a_{max,DB}$. The net breakage rate from monodispersion a=1000 μm.

8. Discretization in drop-size domain

Discretization in drop size distribution into classes always causes error [1]. In our approach this error was avoided by sampling of the distribution at several points (5-25) and using Simpson's integration (3/8 th rule and extended rule depend on number of interval) combined with cubic spline for interpolation between sample points to determine coalescence and breakage rates at each sampling point, fig. 12.

9. Effect of number of sampling points on error and computing time

Fig. 13 shows the effect of the number of sampling points (M) on numerical solution to calculate $\bar{a}(t)$. The step time interval Δt= 1s, and the value of $\bar{a}_o$=1000 μm and $\bar{a}_\infty$=880 μm. As M increases, the error in determining the quasi-equilibrium drop size, $\bar{a}_\infty$=880, will decrease.

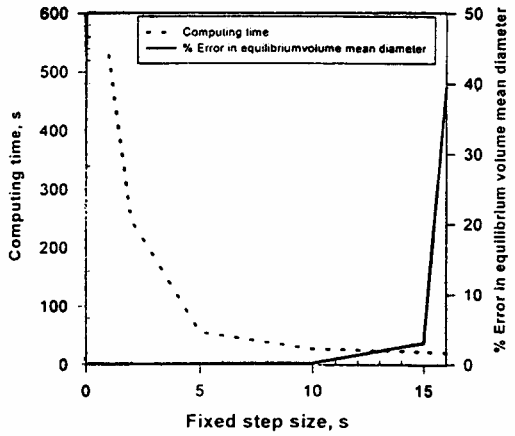

Ks = 1.0E +8; kc = 2.0E-11

Fig. 8. Effect of fixed time step size on computational time and solution error.

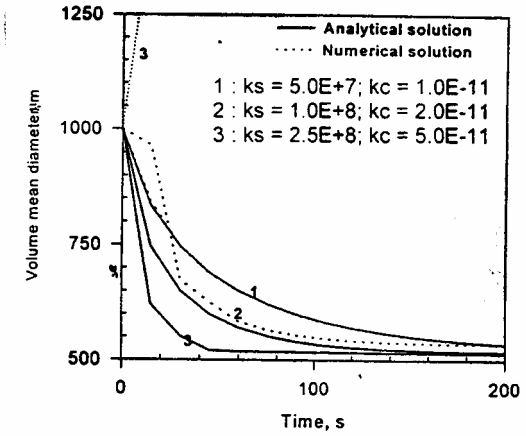

Δt=15 s

Fig. 9. Effect of breakup coefficient on numerical solution.

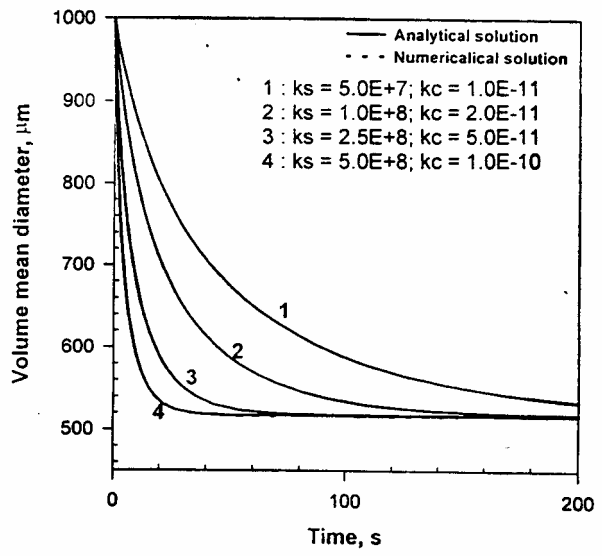

Runge-Kutta 4th order with adaptive step size

Fig. 10.Effect of adaptive time step size on numerical solution.

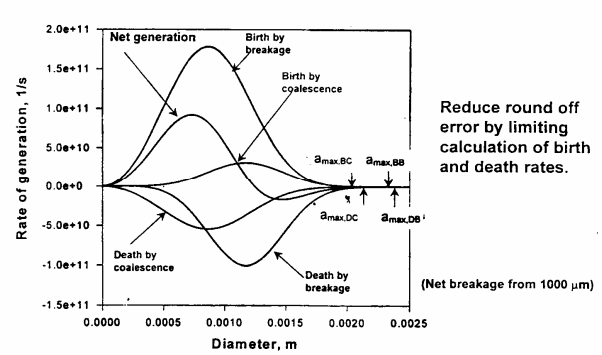

Fig. 11. Limiting the calculation of birth and death rates.

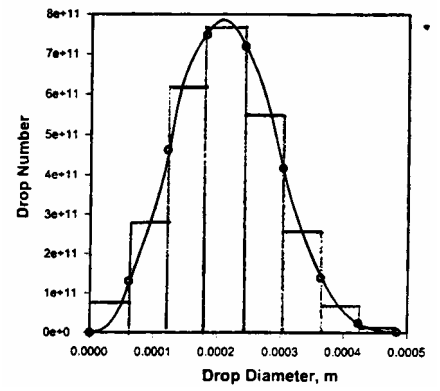

Fig. 12. Discretization in drop-size domain.

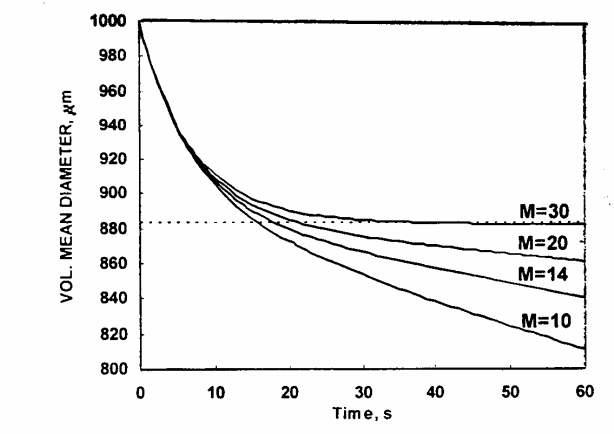

Fig. 13. Effect of M on quasi-equilibrium drop size (net breakage).

Fig. 14 shows the effect of M on the error and computing time of $\bar{a}_{\infty}$, compared with analytical solution. As M increases, the error decreases at the expense of increasing the computing time.

9.1. Adaptive sampling points

As described in fig. 15, the number of the sampling points, M, is not constant, e.g. for distribution 1, M=32, while for distribution 2, M=20. Where distribution 1 could be the initial distribution, and distribution 2 is the final distribution after certain time t, and vise versa.

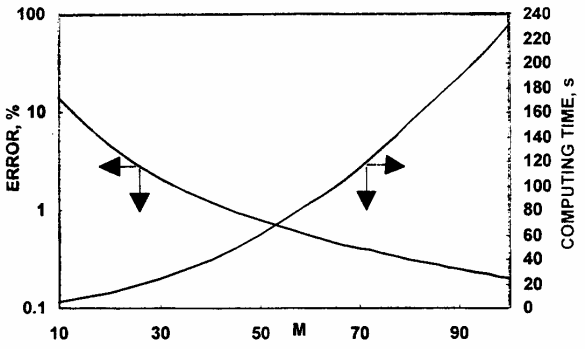

Fig. 14. Effect of M on error and computing time.

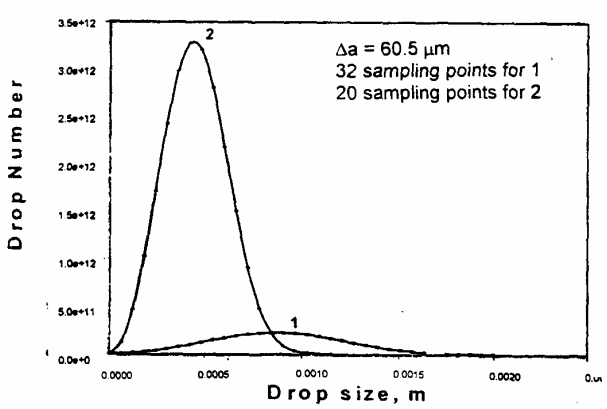

Fig. 15. Adaptive sampling points.

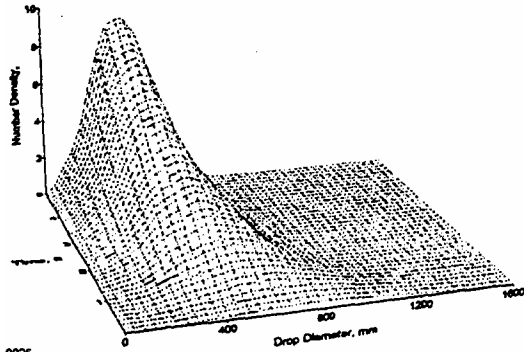

Fig. 16. Temporal variation of drop size distribution.

9.2. Temporal variation of drop size distribution

As shown in fig. 16.

9.3. Solution in short contact time

For high breakage rate, i.e. high k_s, the change in the volume mean diameter in the batch mixer happened quickly, as shown in fig. 17. Using the adaptive numerical method, the numerical solution coincides with the analytical one.

10. Conclusions

High accuracy in solving population balance equations was achieved by using an algorithm that:
i- reduces the error resulting from discretization in the drop size domain (sampling, and integration combined with cubic spline interpolation),
ii- maintains optimum drop size integration range and the number of intervals used to describe the population,
iii- automatically adjusts the step size in the time domain to account for varying the mean drop diameter,
iv- identifies when quasi-steady state is approached.

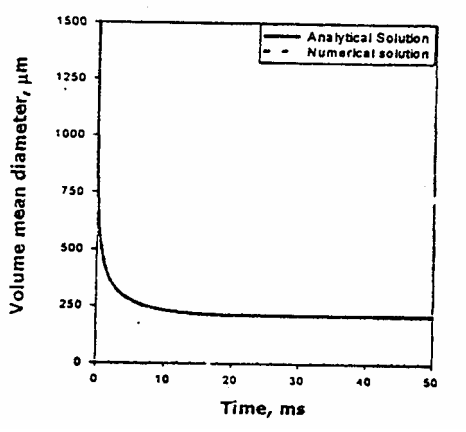

Fig. 17. Comparison between adaptive numerical solution and analytical one for high breakage rate.

Acknowledgement

The financial support of the Royal Thai Government and NSERC is gratefully acknowledged.

Nomenclature

a, a'	is the diameter of drop,
$\bar{a}$	is the volume mean diameter of drop,
a_{max}	is the maximum drop size,
Kc	is the coalescence coefficient,
Ks	is the break-up coefficient,
t	is the time,
$N(t)$	is the total number of particles at time t,
$f(a,t)$	is the fraction of particles have diameter between a and a+Δa,
$B_B(a,t)$	is the birth rate by breakage, of particles of diameter a at time t,
$D_B(a,t)$	is the death rate by breakage, of particles of diameter a at time t,
$B_C(a,t)$	is the birth rate by coalescence, of particles of diameter a at time t,

$D_C(a,t)$ is the death rate by coalescence, of particles of diameter a at time t.
$\varsigma(a')$ is the number of drops formed per breakage of drop of size a'
$\beta(a,a')$ is the number fraction of droplets with size a' formed by breakage of drop of size a
$\Omega(a')$ is the breakage frequency of drop of size a'
$\lambda(a, a')$ is the coalescence efficiency of drops of size a with drops of size a', and
$\omega(a, a')$ is the collision frequency between drops of sizes a and a'
ϕ is the volume fraction of the dispersed phase

References

[1] H. Sovova, "Drop Size Distributions by Power Functions of Breakage and Coalescence", Collection Czechoslovak Chem. Commun. 47, pp. 2393-2402 (1982).
[2] V. Rod, and T. Misek, "Stochastic Modelling of Dispersion Formation in Agitated Liquid-Liquid Systems", Trans. IchemE, Vol. 60, pp.48-53 (1982).
[3] Chung-Hur Lee, L.E. Erickson, and L.A. Glasgow, "Dynamics of Bubble Size Distribution in Turbulent Gas-Liquid Dispersions", Chem. Eng. Comm., Vol. 61, pp. 181-195 (1987).
[4] D. Niyogi, R. Kumar, and K.S. Gandhi, "Modelling of Bubble Size Distribution in Free Rise Polyurethane Foams", AIChE Journal, Vol. 38 (8), pp. 1170-1184 (1992).
[5] E.G. Chatzi, A.D. Gavrielides, and C. Kiparissides, "Generalized Model for Prediction of the Steady-State Drop Size Distributions in Batch Stirred Vessels", Ind. Eng. Chem. Res. 28, pp. 1704-1711 (1989).
[6] D. Ramkrishna, "The Status of Population Balances", Reviews in Chemical Engineering, Vol. 3 (1), pp.49-95 (1985).
[7] C.A. Coulaloglou, and L.L. Tavlarides, "Description of Interaction Processes in Agitated Liquid-Liquid Dispersions", Chemical Engineering Science, Vol. 32, pp. 1289-1297 (1977).
[8] L.L. Tavlarides, and M. Stamatoudis, "The Analysis of Interphase Reactions and Mass Transfer in Liquid-Liquid Dispersions," Advances in Chemical Engineering, Vol. 11, pp. 199-273 (1981).

Received April 10, 2002
Accepted September 12, 2002